Proceedings World Geothermal Congress 2015
Melbourne, Australia, 19-25 April 2015

Effects of Feed Point Configureuration of Wells on Tracer Material Movement in Vertical Two Dimensional Porous Media

Tomohiro Yamashita*, Masahiro Takaki*, Toshiaki Tanaka*, Ryuichi Itoi*

*Department of Earth Resources Engineering, Faculty of Engineering, Kyushu University, Fukuoka 819-0395, Japan

E-mail address, p.sweep00@gmail.com

Keywords: tracer, laboratory experiment, porous media

ABSTRACT

In fault-dominated geothermal reservoirs, productive zones are developed along nearly vertical fracture systems. Wells are drilled to penetrate this fractured zone where feed zones of both production and reinjection wells are located. To simulate the effect of feed point configuration of wells on tracer movement in a fractured system, a laboratory experiment for tracer test was conducted using a vertical two-dimensional porous media by changing depth and horizontal distances of feed points of wells. Color dye was used as tracer chemical in the experiment. Its color intensity was detected at the feed point of production wells and was converted into concentration of dye with a color sensor. Tracer movement in the porous media was visually observed. The optimum number of flow path in the experiment was determined based on the multi-path model using non-linear least squares method.

INTRODUCTION

Reinjection is a common operational strategy during exploitation of water-dominated geothermal reservoirs. This operation is aimed to maintain sustainable production of geothermal fluids as well as to avoid any environmental problems caused by disposing the water into nearby river or stream. However, a quick return of reinjected water to production zones causes temperature drop of reservoir, which eventually decreases steam production of wells.

Tracer tests are conducted in many geothermal areas because it is one of the most effective ways to examine the hydrogeological connection between the production and reinjection areas. The test is conducted by injecting tracer chemicals into the reinjection well and by chemically analyzing the appearance and change of the tracer concentration with time at the production well.

It is recognized that many geothermal reservoirs are characterized with fault system that have nearly vertical dip (Goko. 2000). The presence of this fault system suggests hydrogeological connectivity between production and reinjection areas.

To understand the water flow through the fault system, Sekine et al. (1994) developed a model of underground fractures in the laboratory and performed tracer tests to conduct numerical simulations on tracer response curves.

In this study, we performed laboratory experiments of tracer test using a vertical two-dimensional porous media (Maruo, 2012). In order to visually observe the tracer movement in the model, we injected color dyes as tracer material into injection well. Tracer was detected by optical sensors using an absorption spectrophotometry method for measuring tracer concentration (Takaki, 2013). The sensor can instantaneously detect dyes as tracer in the produced fluid.

In a fault-controlled geothermal system, faults play a role as a reservoir. Tracer test results have been analyzed by applying solute transport equation in one dimensional linear flow system (Axelsson et al., 2005). However, reinjected fluid flow in a high angle fault system where feed zones of reinjection and production wells are located might not be well represented with a linear flow model. Reinjected water flows vertically as well as horizontally in a fault system. To model this two-dimensional flow of tracer chemicals in a porous domain, an experimental apparatus for laboratory studies on tracer test was developed to investigate tracer movement in a vertical two-dimensional porous media. The same setup was used to evaluate the effects of well setup on the tracer concentration obtained in produced fluid when the vertical distances between injection and production wells were varied.

2. LABORATORY EQUIPMENT WITH THE VERTICAL TWO-DIMENSIONAL POROUS MEDIA

Figure.1 shows a picture of the experimental apparatus. Vertical two-dimensional porous media was made up of two 10mm-thick transparent vinyl chloride plates that were placed next to each other. The model has the following final dimensions in mm (LxWxH): 600x20x1500. It was then filled with glass beads of 1 mm diameter. In order to generate homogeneous flow in the porous media, a 150-mm wide entrance region was provided on both sides of the medium.

A total of 20 simulated wells were arranged in five-row and four-column configuration at equal intervals on one surface of the model as shown in Figure.2. The wells were named from W1 to W20 accordingly. With this configuration, the position of the production and injection wells can be located arbitrarily in the experiment.

In the exploitation of geothermal reservoirs, pressure of production zone is generally higher than that of reinjection zone. This was simulated in the experiment by varying the water head difference between the upstream and downstream sides by adjusting the height of the head tanks on both sides of the porous media. This then produces a background flow in the porous media. The water head difference was measured using manometers.

Pumps were attached to simulated production and injection wells. Two solenoid valves separate the tracer flow path filled with tracer from the injection flow path.

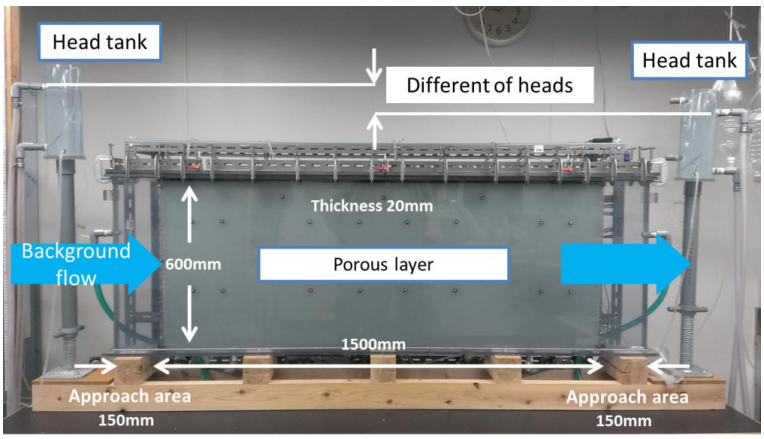

Figure 1: Vertical two-dimensional porous media.

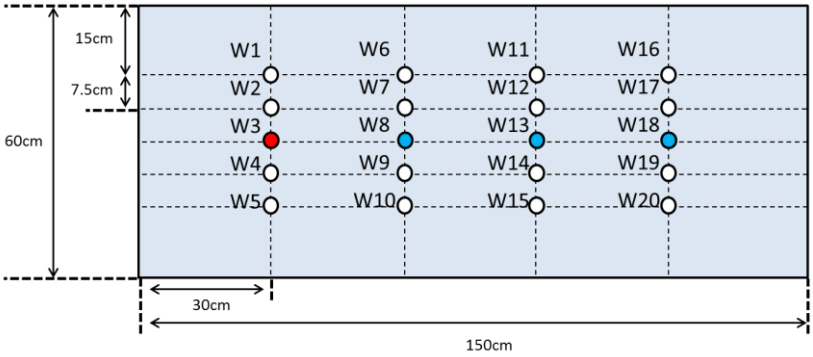

Figure 2: Location of simulated wells in the vertical two dimensional porous media.

3. EXPERIMENTS

To investigate the effects of the distance between production and injection well on tracer curves, different configuration of locations of the wells was given for each experiment. The production well was fixed at W3, and the injection well was placed at three different locations as shown in Figure.2: W8, W13, and W18 to vary the distance between the production and the injection wells at 30cm, 60cm and 90cm, respectively.

After the background flow in the porous media stabilized, the flow rate of the production pump and injection pump was set at 100g/min. A 20mL of 0.1wt% tracers was then filled in the tracer tube section and was injected by switching the solenoid valves one minute after the start of the measurement.

Table 1 Experiment conditions

Experiment Number	Production well (100ml/min)	Injection well (100ml/min)	Distance between production and injection well(cm)
Ex1	W3	W8	30
Ex2	W3	W13	60
Ex3	W3	W18	90

4. RESULTS AND DISCUSSION

Figure.3 presents the tracer response curves at the production well for each experiment. In Ex1, the tracer reached the production well at 300sec. Then, a peak value of 9.32ppm blue tracer concentration was detected at 360sec. Sixty seven percent (67%) of the injected tracer was recovered in the produced fluid for this experiment.

The recovered fraction of tracer was calculated by integrating concentration curves with time as shown in Figure.3. The recovered fraction was calculated using the following equation:

$$S = \int_{t_0}^{t_e} Ca(t) \cdot Gw \cdot \nu \cdot dt \qquad (1)$$

$$f = 100 \times S / Ie \tag{2}$$

where S is the amount of tracer recovered (ppm), $Ca(t)$ is the tracer concentration at time t (ppm/ml), Gw is the production flow rate (ml/min), v is the specific volume of water and t_0, t_e are the starting and ending time (sec) , respectively. Recovery fraction f can be calculated using Equation.(2) where Ie is the injected tracer amount (ppm).

Similarly then, for Ex2, the tracer reached the production well at 1200sec with a peak value of 3.83ppm blue tracer concentration detected at 1680 sec. The recovered fraction of tracer was calculated at 55%.

In Ex3, the tracer reached the production well at 3400sec. and a peak value of 0.90ppm blue tracer concentration was detected only after 4860 sec. The recovered fraction of tracer was calculated at 37%.

Among the three experiments, tracer of Ex1 has the highest measured concentration value and it was detected at the earliest time at production well. Conversely, tracer of Ex3 has the lowest concentration and it was detected at the latest time. Moreover, as shown from Figure.3, tracer concentration in Ex1 decreased quickly as compared to the slow decrease in tracer concentration with time for Ex3. As distance between production and injection well becomes longer, tracer response curve becomes broader. Tracer becomes more dispersed as the distance between production and injection well becomes longer; thus having a low detected concentration value when it reaches the production well.

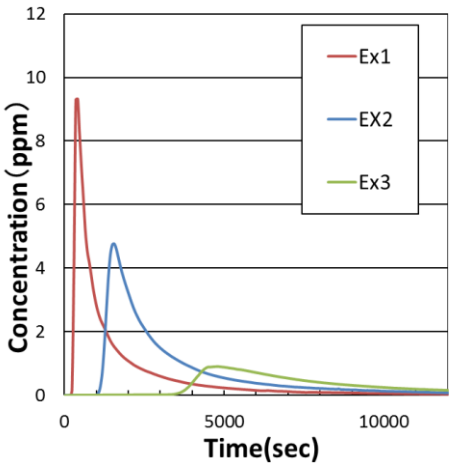

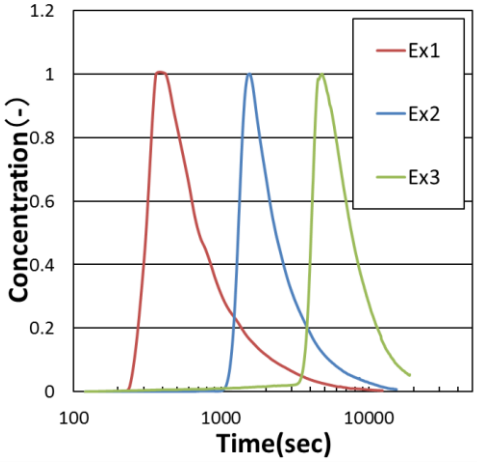

Figure 3: Tracer concentration curves at the production well. **Figure 4: Tracer concentration curves at the production well (Non-dimensional semi-logarithmic graph).**

Figure.4 presents the non-dimensional semi-logarithmic graph of tracer response curves. The vertical axis of Figure.4 is the ratio of each tracer concentration with the peak of the tracer curve. The horizontal axis of Figure.4 is expressed as the logarithm of time.

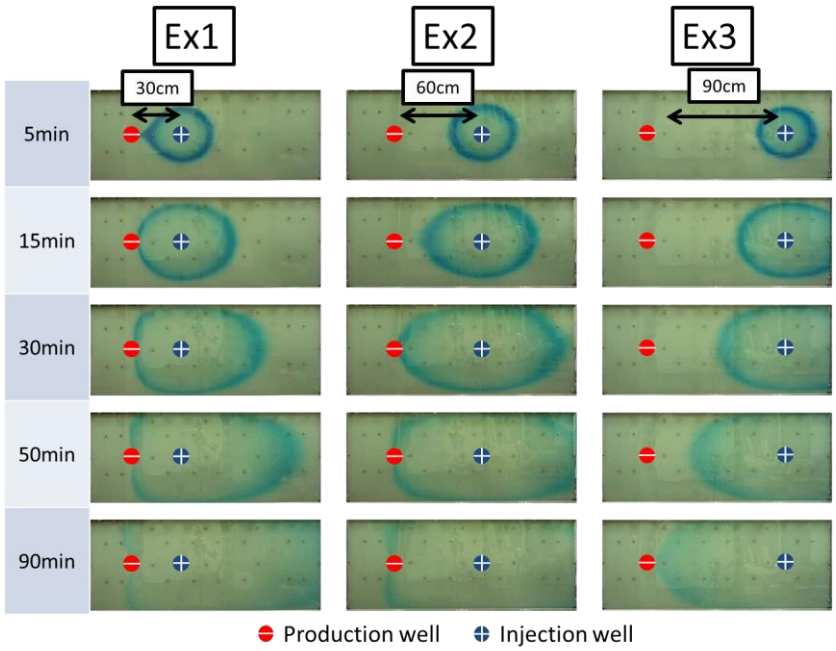

Figure 5: Pictures of tracer movement in the porous media with time during each experiment.

Unlike in Figure.3, each tracer curve in Figure.4 has almost identical form with the other tracer curves. Since the experiments conducted here only differed in the distance between production and injection wells, the similar form in the concentrations suggests that the tracers may have either flowed through the same path or they may have flowed through paths which have similar hydraulic characteristics. Thus, by changing to non-dimensional semi-logarithmic graph, we can know whether each tracer flows in similar zone or not.

Figure.5 shows pictures of tracer movement in the porous media during each experiment. Each tracer flows toward the production well and through the downstream along the top and bottom part of the porous media, which acted as impermeable boundaries; where hence the tracer stayed at these impermeable boundaries for a long time.

5. ANALYSIS OF EXPERIMENT RESULTS WITH A LINIER FLOW MODEL

5.1. Multiple-path model

In this study, we used the multi-path model developed by Tanaka et al. (1997), which assumes a minimum number of paths between the injection and production wells and calculates each tracer recovery curve on the basis of several parameters such as recovery fraction, average residence time, and Peclet number. The combined tracer recovery curves were then fitted with the observed curve.

The basic convection-dispersion equation in one dimensional line flow system used in this study is as follows:

$$D\frac{\partial^2 C}{\partial x^2} - V\frac{\partial C}{\partial x} = \frac{\partial C}{\partial t} \tag{3}$$

where D is the dispersive coefficient (m^2/h), C is the tracer concentration (mg/l), and V is the average velocity in the path (m/h).

Equation.(3) can be solved under the following initial and boundary conditions:

1. $x \geq 0,\ t = 0 \qquad C=C_0$
2. $x = 0,\ 0 < t < t_1 \quad C=C_I$

   $x = 0,\ t \geq t_1 \qquad C=C_0$

   $x \to \infty,\ t > 0 \qquad C=C_0$

where C_0 is the background concentration (mg/l). t_1 is the injection time(h) of the tracer, and C_I is the tracer concentration (mg/l).

Then, the analytical solution of Equation.(3) is expressed as follow;

$$C^* = \frac{1}{2}\left[\left\{erfc\left(\frac{a-t}{2\sqrt{(a/Pe)t}}\right) + \exp(Pe)\cdot erfc\left(\frac{a+t}{2\sqrt{(a/Pe)t}}\right)\right\} - erfc\left(\frac{a-(t-t_1)}{2\sqrt{(a/Pe)(t-t_1)}}\right) + \exp(Pe)\cdot erfc\left(\frac{a+(t-t_1)}{2\sqrt{(a/Pe)(t-t_1)}}\right)\right] \tag{4}$$

$$erfc(x) = 1 - erf(x) = 1 - \frac{2}{\sqrt{\pi}}\int_0^x e^{-t^2}dt \tag{5}$$

$$C^* = \frac{C-C_0}{C_I-C_0}, C_I = C_0 + \frac{I}{G_I v_I t_I} \tag{6}$$

$$a = x/V \tag{7}$$

$$Pe = Vx/D \tag{8}$$

where a is the average residence time of the fluids (h), Pe is defined as a function of mobility ratio (Peclet number) (-), C_I is the tracer concentration (mg/l), and I is the amount of tracer (kg). In Equation.(5), erf(x) is the error function and erfc(x) is the complementary error function.

In case where there are n flow paths, the tracer concentration at production well (C_S^*) is calculated as follow:

$$C_S^* = \frac{G_I v_I}{G_w v_w}\sum_{i=1}^{n} f_i C_i^*$$
$$\sum_{i=1}^{n} f_i \leq 1 \tag{9}$$

where G_I is the amount of injected water (kg/h), v_I is the specific volume of injected water, G_w is the amount of produced hot water (kg/h), v_w is the specific volume of produced hot water, f_i is the reproduced ratio of each flow path and C_i is the tracer concentration of each flow path(mg/l).

5.2. Optimum flow path number

In calculating non-dimensional tracer concentration (C^*) from measured tracer concentration (C), and in determining unknown parameters through non-linear least squares method, an optimum flow path number in the model must be determined. In this study, the flow path number becomes optimum when the residual sum of squares between the measured value and calculated value becomes minimum. The smallest possible number of flow paths at that time is then considered to be the optimum flow path number in the model.

We used *AIC* (Akaike's Information Criterion) as evaluation criteria. It is defined as follow:

$$AIC = n\ln(LRSS) + 2r \tag{10}$$

where n is the number of data, *LRSS* is the least residual sum of squares and r is the number of unknown parameter. Calculating and comparing the AIC for several flow paths (n), the flow path number which gives the least AIC value is considered as the optimum flow path number. However, this optimum flow path number does not necessarily indicate the real flow path number but instead is a discrete representation of the number of flows the tracer has traveled in the model.

5.3. Analysis of experiments results and discussion

Figureure6 presents the relation between flow path number and AIC for Ex1, Ex2 and Ex3, respectively. Optimum number of flow path was determined to be 7, 7, and 5 for Ex1, Ex2, and Ex3, respectively. The optimum number of flow path decreases with increasing distance between the wells.

Tracer concentration measured at production well for Ex1 is plotted in green square in Figure.7. The analyzed result for the curve shows seven (7) flow paths. The concentration results due to each flow path are also plotted in Figure.7. Among these return curves, sharp concentration peaks appear for path1 to 4. These are the paths with high Peclet number and low average residence time. This implicitly suggests that the dominant flow in these paths is through convection. In contrast, broad concentration curves as in path 5 to 7 have low Peclet number and high average residence time. This means that a diffusion-dominant flow occurs along these paths. Concentration curves of the seven different paths are summed up in Figure.7. This cumulative sum as indicated by *pathsum* in the Figure shows a good agreement with the measured values.

Figure.8 presents estimated parameters (a_i, f_i, Pe_i) with least AIC value. In general, estimated values of f and a increase while Pe decreases with an increase of flow path number. Smaller values of Pe suggest that tracer transport is diffusion-controlled.

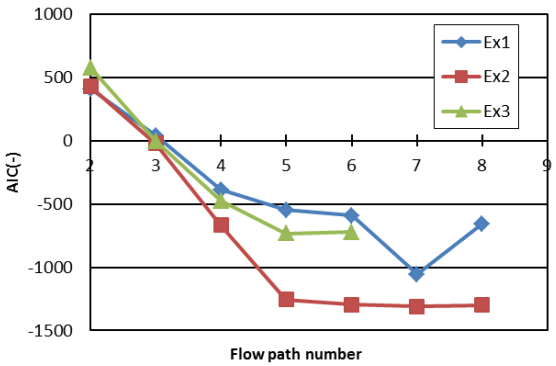

Figure 6: Relation between flow path number and AIC

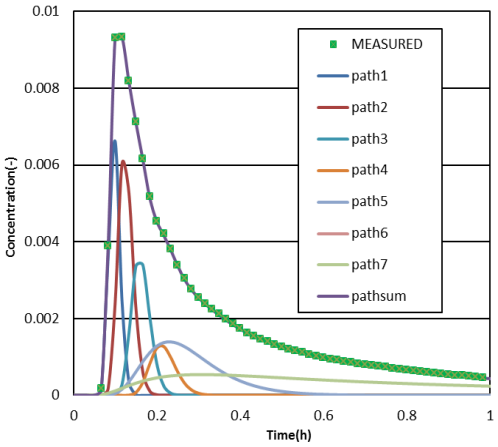

Figure 7: Result of experiment analysis (Ex1).

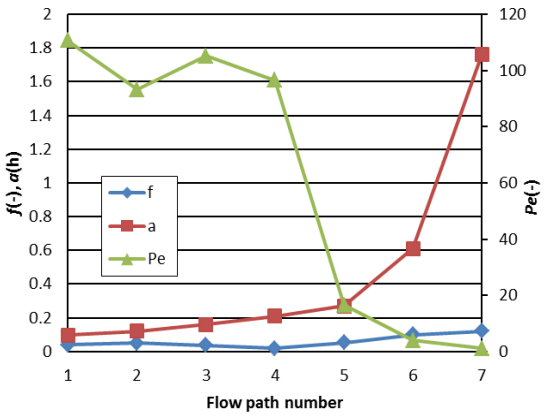

Figure 8: Estimated parameter of each flow path (Ex1)

In this paper, we focused on the average residence time of the fluids, *a*. We suppose there are two paths from the injection well to production well as shown in Figure.9. One of the paths has a distance of *L*(m), velocity of *V*(m/s) and residence time of *a*. Another path has distance of $n \times L$ (m) where *n* is the ratio of flow path length from IW to PW. The velocity (m/s) of the longer path is obtained by Darcy's law as expressed in Equation.(11):

$$V = -\frac{k}{\mu} \cdot \frac{\Delta P}{L'} \tag{11}$$

where *k* is the permeability(m^2), μ is the viscosity (Pa·s), ΔP is the pressure difference between the injection well and the production well, and *L'* is the flow path length. The velocity (m/s) of the longer path is then shown as *V*/*n* (m/s) and the average residence time in this path is $nL/(V/n)=n^2a$. As a result, for the same pressure difference value, the flow path length between IW and PW increases *n* times and the average residence time increases by a factor of n^2.

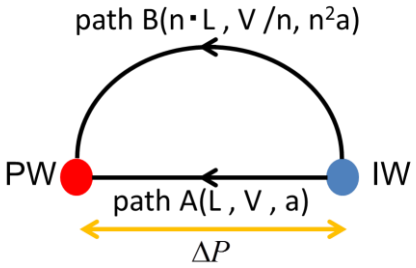

Figure 9: Relation between distance, velocity and average residence time

Figure.10 presents the average residence time, *a* of paths 1, 2, 3 and4 for each experiment. Because the average residence time increases n^2 times when the flow path length between IW and PW increases *n* times, we assumed that the average residence time is in proportion to *n* to the power of *k* as follow:

$$\begin{aligned} a_2 &= n_{12}{}^k \cdot a_1 \\ a_3 &= n_{13}{}^k \cdot a_1 \end{aligned} \tag{12}$$

n_{12}(=2) and n_{13}(=3) are taken as the ratio between the distance of the wells in Ex1 at 30cm and Ex2 at 60cm, and Ex1 and Ex3 at 90cm, respectively. Substituting n_{12} and n_{13} to Eq.(12), we obtain Eq.(13):

$$\begin{aligned} a_2 &= 2^k \cdot a_1 \\ a_3 &= 3^k \cdot a_1 \end{aligned} \tag{13}$$

We deal with the least residual sum of squares (LRSS) as follow:

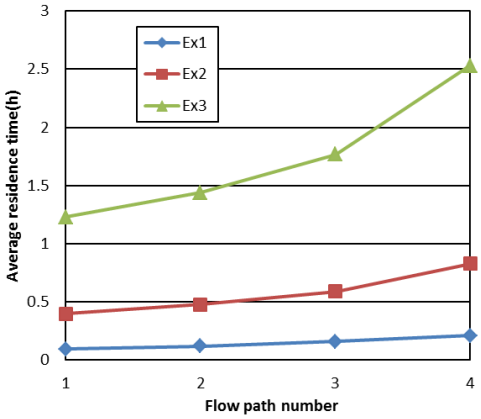

Figure 10: Average residence time (a) of path1, 2, 3 and 4 of each experiment.

$LRSS^* = LRSS_{12} + LRSS_{13}$

where $LRSS_{12}$ is the least residual sum of squares between $2^k a_1$ and a_2 , and $LRSS_{13}$ is the least residual sum of squares between $3^k a_1$ and a_3. The optimum value of *k* is determined when LRSS* becomes minimum.

Following this process, the value of k is calculated as 2.17. Thus, a_2 and a_3 becomes Eq.(14):

$$a_2 \fallingdotseq 2^{2.17} \cdot a_1$$
$$a_3 \fallingdotseq 3^{2.17} \cdot a_1 \quad (14)$$

Consequently, in two-dimensional flow, the average residence time increases in proportion to the ratio of distance from IW to PW to the power of 2.17.

6. CONCLUSIONS

In this study, assuming the vertical two-dimensional porous media to be a high dip fault, we conducted three experiments with varying horizontal distance between injection and production wells in the porous media. We detected tracer at the production well in each experiment. From the result of the tracer experiments, we obtain the following information:

1. Tracer response curve becomes broader as distance between production and injection well becomes longer.
2. Each tracer curve follows the same form when plotted on the semi-logarithm paper with logarithm of time.
3. Response curves of tracer which flow in two-dimensional domain was analyzed by multi-path model. The measured values have good agreement with the cumulative sum of the different flow paths determined in the multi-path model.
4. Average residence time is proportional to square of the ratio of flow path length.

REFERENCES

Axelsson, G., Bjornsson, G., Montalvo, F., : Quantitative Interpretation of Tracer Test Data, Proc. World Geothermal Congress 2005,(2005).

Goko, K.: Structure and hydrology of the Ogiri field, West Kirishima geothermal area, Kyushu, Japan, Geothermics, v. 29, (2000),127-149

Kumagai, N., T. Tanaka, and K. Kitao, : Characterization of geothermal fluid flows at Sumikawa geothermal area, Japan, using two types of tracers and an improved multi-path model, Geothermics, v. 33, (2004), 257-275

Maruo, T., R. Itoi, T. Tanaka, M. Iwasaki, H. Oishi, : Laboratory experiment of tracer test with vertical two-dimensional porous media, Proc. International Symposium on Earth Science and Technology, (2012), 141-145

Sekine, H., H. Fukunaga, S. Toyoda.: Identification of Extent of Underground Fractures by Use of Tracer Response -Fundamental Research Conducted by Using Models of Underground Fractures-, Journal of the Geothermal Research Society of Japan, v. 16, no.1, (1994), 109-126

Takaki, M., R. Itoi, T. Tanaka, T. Maruo, : Laboratory experiment of tracer test in the vertical two-dimensional porous media with newly developed tracer sensors, Geothermal Resource Council ,v. 37, (2013), 337-340

Tanaka, T., Nakamura, H., Itoi, R. and Fukuda, M. : An analysis method of tracer by using genetic algorithms and its application, Proc. the World Geothrmal Congress,(2000),1869-1874